*J. Fluid Mech.* (1971), *vol.* 47, *part* 4, *pp.* 779–787
*Printed in Great Britain*



# Convective instability in liquid pools heated from below

By HARVEY J. PALMER AND JOHN C. BERG

Department of Chemical Engineering,
University of Washington, Seattle, Washington 98105

(Received 29 June 1970 and in revised form 6 January 1971)

The linear hydrodynamic stability analysis of liquid pools heated from below combining surface tension and buoyancy effects as presented by Nield (1964) is confirmed by experiment for a series of silicone oils. The experimental method used is an adaptation of the Schmidt–Milverton technique, in which the stability limit is located by the change of slope in the plot of heat flux versus temperature drop across the liquid pool.

## 1. Introduction

A quiescent fluid heated from below becomes stratified with respect to its various fluid properties as a result of their dependence upon temperature. The forces to which the fluid is subject, usually gravity and surface forces acting alone or in concert, may render the stratification unstable. The quiescent but unstably stratified fluid, being continually subject to microscopic disturbances, will eventually give way to convective flow, sometimes in the form of regular hexagonal cells as observed in the classical experiments of Bénard (1901).

Gravity induced convective instability, caused by vertical density stratification, is common in many heat transfer systems and has been extensively investigated both theoretically and experimentally. Theoretical values of critical Rayleigh numbers have been reported for systems subject to various hydrodynamic and thermal boundary conditions, as summarized elsewhere (Berg, Boudart & Acrivos 1966). Systems bounded at both top and bottom by solid surfaces are subject to gravitational forces only. For this case, and with isothermal boundaries at top and bottom, theory predicts a critical Rayleigh number $R = g\alpha d^3\Delta T/\kappa\nu$, of 1708, where $g$ is the gravitational acceleration, $\alpha$ thermal expansivity, $d$ liquid depth, $\Delta T$ temperature drop, $\nu$ kinematic viscosity and $\kappa$ thermal diffusivity. Experiments, particularly those of Silveston (1958), later yielded a value of $1700 \pm 40$ providing a striking confirmation of the linear hydrodynamic stability analysis.

When a pool of liquid with a hydrodynamically free upper surface is heated from below, surface tension forces as well as buoyancy forces become important. The case for which surface forces alone govern the stability of the system was first solved by Pearson (1958) yielding a stability parameter now called the Marangoni number, $Ma = -(d\sigma/dT)\,d\Delta T/\mu\kappa$, where $\sigma$ is the surface tension and $\mu$ dynamic viscosity. Its critical value is 80 for the case of an isothermal

lower boundary and a constant flux boundary at the upper surface. Pearson's results extend to other thermal boundary conditions as well.

Nield (1964) analyzed the situation in which both surface forces and gravity-dependent buoyancy forces are present and thus combined the Rayleigh and Pearson analyses. The critical Marangoni number in a given situation was found to be roughly inversely proportional to the Rayleigh number of the system, and vice versa, as shown by the solid line of figure 5 below. The Marangoni numbers on Nield's plot are normalized by the critical values, $Ma^*$, that apply in the absence of buoyancy effects and the Rayleigh numbers are normalized by the corresponding critical values, $R^*$, that apply in the absence of surface tension effects.

Almost concurrent with the publication of Nield's results, there appeared two modifications of the Pearson analysis (hence also of the Nield analysis). First, Scriven & Sternling (1964) relaxed Pearson's somewhat artificial restriction to a rigid upper surface and found much lower critical Marangoni numbers, but only for large wavelength disturbances. In the range of moderate disturbance wavelengths, Pearson's criterion remains essentially unchanged. Secondly, Berg & Acrivos (1965) analyzed the effect of surface active agents on systems subject to surface tension forces and found that the critical Marangoni number increases by as much as eight orders of magnitude in the presence of even trace amounts of these materials. Berg & Acrivos found that although the buoyancy mechanism remains operative, the appropriate hydrodynamic boundary condition at the upper surface is closer to that of a solid surface than a free surface.

In contrast to the case of gravity induced instability in a liquid layer confined between solid surfaces, none of the criteria of instability in pools of liquid (with a free upper surface) has received experimental confirmation. Although rough qualitative agreement between experimental observation and the results of linear stability analysis involving surface forces has been suggested, no quantitative stability data have been reported. The primary objective of the present work was, therefore, to obtain such data for a number of different liquids, and to make comparison with the present theory as expressed by Nield. It was of particular interest to inquire into the effect of gradually increasing the pool depth and to examine the expected transition from surface tension dominated breakup to gravity dominated breakup of the quiescent liquid layer.

Finally, the theoretical work of Scriven & Sternling (1964) and Berg & Acrivos (1965) have each raised a serious question about the relevance of the traditional model of the liquid surface to actual experimental conditions. The former suggests that free surface deformability may render the pool *unstable* under virtually all conditions, provided sufficiently large wavelength disturbances are present, while the latter suggests that free surface contamination may render the pool *stable* under a much widened range of conditions, provided trace surface contamination is present. Experimental determination of free surface stability criteria under a range of conditions should establish the importance of these effects.

## 2. Experimental technique

The experimental method chosen for determining the criteria for instability in liquid pools heated from below was an adaptation of the Schmidt–Milverton technique for detecting instability in fluid layers between solid plates (Schmidt & Milverton 1935). The fluid under study is confined between a pair of horizontal plates, and a steady-state temperature gradient across the liquid layer is obtained by heating the bottom plate while the top plate is cooled. The temperature difference across the fluid layer is changed by increasing or decreasing the heat flux to the bottom plate. When the heat flux across the fluid layer is plotted

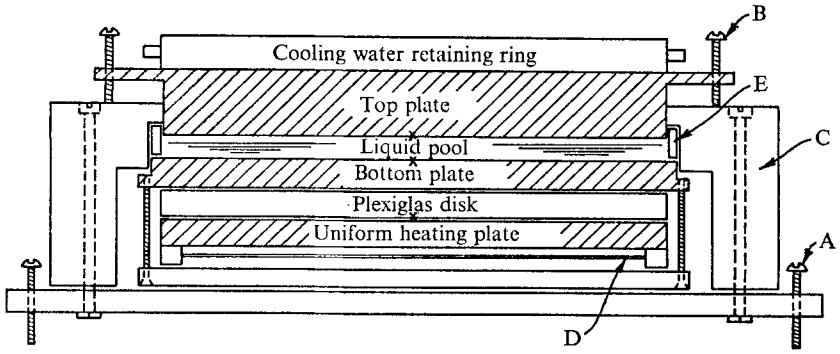


FIGURE 1. Schematic diagram of apparatus.

against the temperature difference between the plates, a straight line of slope $k/d$ is obtained for the quiescent régime, where $k$ is the thermal conductivity of the liquid and $d$ its thickness. When the stability of the fluid layer collapses, however, heat is transferred across it by convection as well as conduction, and a rather sharp increase in the slope of the heat flux versus temperature difference plot is obtained, identifying the stability limit. This technique has been used successfully in the study of single fluid layers in contact with solid surfaces not only in the location of the stability limit but in the determination of subsequent transitions in the convective mode as heat flux is increased (cf. Silveston 1958).

In the present adaptation, described in detail below, the liquid layer does not fill the entire space between the solid plates; a thin vapour space separates the free liquid surface from the top plate. Figure 1 shows a vertical cross-section o the apparatus, the principal components of which are the top and bottom aluminium plates, 9 in. in diameter and 1 in. and $\frac{1}{2}$ in. thick, respectively; a Plexiglas disk, $\frac{1}{2}$ in. thick; an aluminium heating plate, $\frac{1}{2}$ in. thick; and a Nichrome wire heater at the bottom and a cooling water retaining ring at the top.

The Teflon gasket (E), which retains the liquid pool, provides a liquid-tight seal between it and the bottom plate. The gasket also prevents contamination of the liquid by the Plexiglas framework. The liquid depth is measured at the centre and at various points around the periphery of the layer with a microscrew suspended over the surface. The microscrew consists of a needle mounted onto the jaw of a micrometer caliper. The needle point is lowered until it meets the

liquid surface, the position recorded, and then the point is lowered further until it meets the floor of the vessel, where the position is again recorded. The liquid depth can thus be measured to within $\pm 0{\cdot}001$ in. Any variation in liquid depth indicates that the bottom plate is not horizontal and that a slight adjustment of the levelling screws (A) is required.

The liquids used in this study were a series of the Dow–Corning 200 silicone oils (see table 1). These liquids were chosen for their non-volatility and particularly for their low surface tension, which would, it was hoped, keep them free of surfactant contamination. They were degassed before each run by heating them for at least one hour at 90 °C. After the liquid had been placed in the apparatus, the top plate was lowered into position by means of its supporting

| | | | |
|---|---|---|---|
| Kinematic viscosity (centistokes) | 200 | 50 | 10 |
| Specific gravity | 0·971 | 0·960 | 0·940 |
| Coefficient of expansion ($cm^3/cm^3$ °C) | 0·00096 | 0·00104 | 0·00108 |
| Thermal conductivity (cal/sec $cm^2$ °C/cm) | 0·00037 | 0·00036 | 0·00032 |
| Specific heat (cal/g °C) | 0·35 | 0·36 | 0·425 |
| Surface tension (dynes/cm) | 21·0 | 20·8 | 20·1 |
| Surface tension–temperature coefficient (dynes/cm °C) | −0·068 | −0·068 | −0·068 |

Data obtained from Bulletin 05-136 of Dow Corning, Engineering Products Division (1965).

TABLE 1. D.C. 200 fluid properties at 25 °C

screws (B) until there was only a small, uniformly thin, air gap between the top plate and the liquid surface. The thickness of the air gap was determined by subtracting the liquid depth from the overall distance between the top and bottom plates. The overall gap height was obtained by measuring, with the microscrew, the distance between the top plate flange and the top of the Plexiglas ring (C) when the top and bottom plates were in contact with each other, and again, when the liquid was in place and the top plate had been lowered into position. Liquid pool depths were varied between 0·24 mm and 1·03 cm, while the air gap varied in thickness between 0·15 and 0·31 cm.

The experiment consisted of determining the steady-state curve of heat flux versus the temperature difference across both the liquid and the air between the plates. The bottom plate was heated electrically with a heater made of Nichrome wire woven through a perforated asbestos board. The magnitude of the heat flux through the fluid layer was increased a small amount for each data point by increasing the electrical power input to the heater with a Variac. A plate of aluminium was placed above the heater to smooth out any lateral temperature gradients that might have existed just above the heater itself. Cooling water, maintained at a constant temperature to within $\pm 0{\cdot}02$ °C, was circulated over the top plate to remove heat from the upper surface of the gap. The possibility of non-uniformities in the surface temperatures of both the top and bottom plates was checked with thermocouples placed radially outward from the centre of each plate; no temperature variations were detected. Heat losses to surroundings were minimized by encasing the entire apparatus with

eight-inch thick Styro-foam insulation. To correct for remaining heat losses, the temperature of the outside of the apparatus was monitored on opposite sides with two thermocouples attached to a metal sleeve around the apparatus.

The heat flux through the fluid layer was determined by measuring the temperature drop across the Plexiglas disk ($\Delta T_p$) below the bottom plate, and was given by

$$q = h_{\text{eff}} \Delta T_p + c, \tag{1}$$

where $h_{\text{eff}}$ is the effective heat transfer coefficient of the Plexiglas disk and $c$ is a constant representing the rate of heat loss in each experiment. The behaviour of $h_{\text{eff}}$ and $c$ was determined by making numerous runs in which the fluid layer consisted of air alone or oil alone and in which the temperature drop across the gap was kept well below the critical value for Rayleigh instability. It was found that $h_{\text{eff}}$ was a constant under all conditions and that $c$ was constant in any given experiment. Finally, experiments were run, with oil filling the entire gap, in which the critical temperature drop for Rayleigh instability was reached and exceeded. An average critical Rayleigh number of 1750 was obtained, in good agreement with the theoretical value of 1708.

The direct proportionality of the heat flux in each case to temperature drop across the Plexiglas disk meant that the stability limit for the system could be determined from the discontinuity in the graph of $\Delta T_p$ versus the temperature drop across the liquid–air layer, $\Delta T_{LA}$. Precise knowledge of the heat flux was needed only in the heat transfer analysis of the post-convective régime, which is to be reported elsewhere. The temperature differences, $\Delta T_p$ and $\Delta T_{LA}$ were the primary data required for construction of the stability diagram. These temperature differences were measured with pairs of precision thermistors embedded in the aluminium plates at the points shown by crosses in figure 1. The log of the ratio of the resistances of two matched thermistors is proportional to the temperature difference between them,

$$\ln \frac{R_2(T_2)}{R_1(T_1)} = b \left( \frac{T_1 - T_2}{R_1 T_2} \right), \tag{2}$$

where $T$ is in units of absolute temperature and $b$ is a constant. This resistance ratio was measured by means of a Wheatstone bridge which permitted measurement of temperature differences with much greater precision ($\pm 0{\cdot}02\,^{\circ}\text{C}$) than if the thermocouples had been employed. However, thermocouples were used to measure the absolute temperatures in the system to $\pm 0{\cdot}1\,^{\circ}\text{C}$ for determination of physical parameters, as well as to drive a chart recorder, which provided a visual means for following the system's slow approach to steady state. After the electrical input to the heater had been re-set, the system required between 3 and 6 h to re-establish steady-state conditions.

While the break in the curve of heat flux (or $\Delta T_p$) versus the temperature drop across the entire liquid–gas layer heralded the onset of convection, the temperature drop across the liquid pool alone had to be determined in order to evaluate the stability parameters, $R$ and $Ma$. The temperature drop across the thin air gap, which must be subtracted from the total temperature drop, was readily obtained because the air gap was always stagnant prior to the onset of

convection. It is likely that the air gap, the Rayleigh number of which never exceeded a value of 15, remained virtually stagnant even after the onset of convection in the liquid pool below. In the pre-convective state, the temperature drop across the air gap, $\Delta T_A$ was thus given by

$$\Delta T_A = \frac{q d_A}{k_A} = \Delta T_{LA}\left(1+\frac{k_A d_L}{k_L d_A}\right)^{-1}, \tag{3}$$

where $\Delta T_{LA}$ is the total temperature drop across the liquid–air layer and subscripts $A$ and $L$ refer to air and liquid, respectively. The temperature drop across the liquid pool was then given by $\Delta T_L = \Delta T_{LA} - \Delta T_A$. In the post-convective state, $\Delta T_A$ was computed with the assumption that the air layer remained stagnant.

Schmidt–Milverton diagrams, as shown in figures 2–4, were constructed showing $\Delta T_p$ (proportional to heat flux) versus $\Delta T_L$, as calculated above. Least squares fits were obtained for the pre-convective and post-convective data separately to obtain two straight lines whose intersection defined the critical value of $\Delta T_L$, and from this the critical Marangoni and Rayleigh numbers were calculated. It should be noted that whether the assumption of a stagnant air gap in the post-convective régime is correct or not, the value of $\Delta T_L$ at the critical point, as determined above, remains essentially unaffected. Any convection that commenced in the air gap when convective instability appeared in the liquid would change only the slope of the upper branch of the Schmidt–Milverton curve, and not the location of the break point.

## 3. Results and discussion

The experimental results are shown in figures 2–5 and table 2. $Ma_c$ and $R_c$ are the maximum values of the Marangoni and Rayleigh numbers at which the liquid pool remained stagnant. In table 2, $Ma^*$ represents the expected critical Marangoni number if buoyancy forces are absent (cf. Pearson 1958), and $R^*$ is the critical Rayleigh number in the absence of surface forces, (cf. Sparrow *et al.* 1964). The values for $Ma^*$ and $R^*$ varied from one run to the next because of their dependence on the Biot number, $L = k_A d_L / k_L d_A$, which changed with the fluid depth and with different fluids.

The results are best compared with theory by plotting them on Nield's stability diagram (figure 5). The solid line corresponds to the case of $L = 0$; Nield's full results show a very weak dependence of the stability criteria on the Biot number. In the present experiments $L$ varied but was always less than unity, which is very small. The comparison between the experimental and the theoretical stability criteria is sufficiently good to substantiate the validity of Nield's hydrodynamic stability analysis. More importantly, the results validate the use of the non-deformable, non-contaminated model of the liquid surface, at least for the series of silicone oils and the experimental conditions studied. The pools, of course, were not infinite in horizontal extent (the width was 23 cm), so that extremely large wavelength disturbances were geometrically excluded

from the system. It is in the stability of the system toward such disturbances that free surface deformability has its greatest predicted effect.

The precision with which experimental values of $Ma_c$ and $R_c$ could be determined depended in each case upon the distinctness of the break in the plot of $\Delta T_p$ versus $\Delta T_L$. Error analysis indicated that while individual temperature differences were accurate to within $\pm 0{\cdot}02\,°C$, the derived critical values of $\Delta T_L$

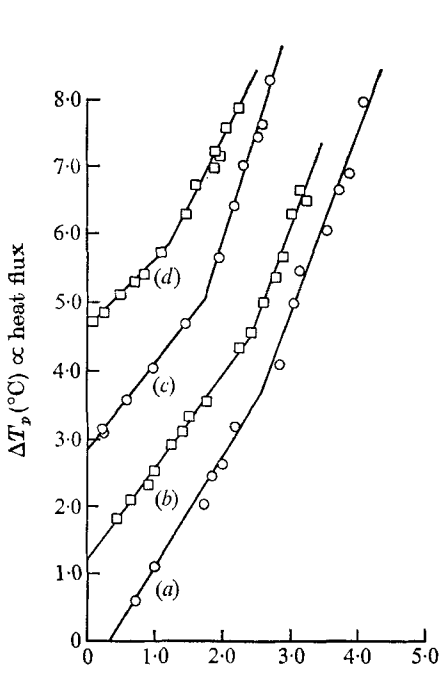


FIGURE 2

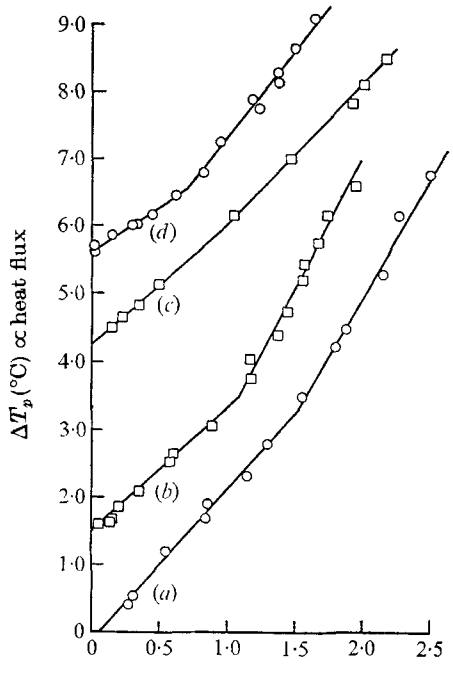


FIGURE 3

FIGURE 2. Heat flux versus temperature drop across pools of 200 centistoke silicone fluid. Curves (*a*)—(*d*) represent pool depths of 5·72, 6·63, 7·39 and 10·29 mm, respectively, and curves (*b*)–(*d*) are displaced upward by 1·5, 3·0, and 4·5 °C, respectively.

FIGURE 3. Heat flux versus temperature drop across pools of 50 centistoke silicone fluid. Curves (*a*)–(*d*) represent pool depths of 3·81, 4·62, 5·46 and 6·55 mm, respectively, and curves (*b*)–(*d*) are displaced upward by 1·5, 4·5 and 5·5 °C, respectively.

could be determined only to within $\pm 0{\cdot}1\,°C$ to $\pm 0{\cdot}2\,°C$. The relative effect of this uncertainty on $Ma_c$ and $R_c$ depends on the magnitude of the critical value of $\Delta T_L$. Since this was as low as 0·44 °C, for the shallowest depth of the 10 centistoke fluid, the effect could be quite severe. The low values of $\Delta T_L$ required to bring about instability in liquid pools compared with the values required for liquids confined between solid plates makes study of the former case much more exacting. A specific example is instructive. For a 2 mm deep pool of the 10 centistoke silicone oil, the combined surface tension-buoyancy stability analysis predicts the onset of convection when $\Delta T_L$ reaches 0·42 °C, corresponding to $Ma = 75$ and $R = 44$. On the other hand, if the same liquid were confined between solid plates, the predicted critical Rayleigh number would

be 1708, leading to a critical $\Delta T_L$ of 16·2 °C. The experimental uncertainty of ± 0·1 °C to ± 0·2 °C has a much more drastic effect on the free surface case. Figure 5 shows all of the stability data obtained, and none departs from the theoretical curve by more than the experimental precision allows.

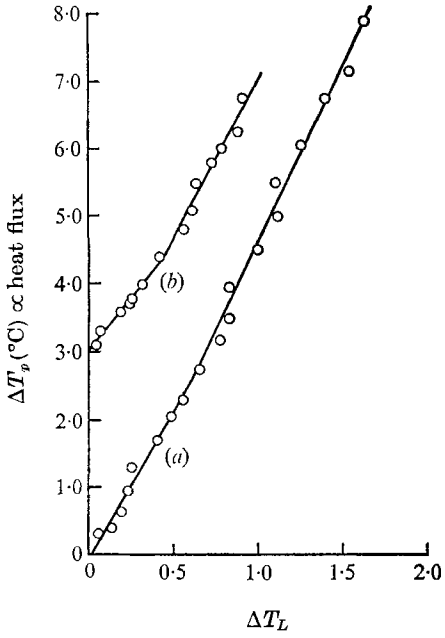


FIGURE 4

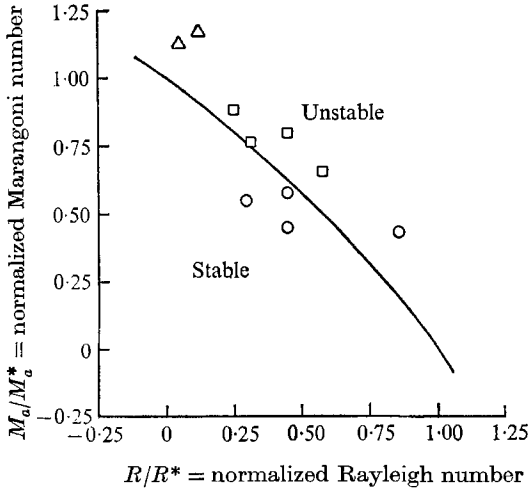


FIGURE 5

FIGURE 4. Heat flux versus temperature drop across pools of 10 centistoke silicone fluid. Curves (*a*) and (*b*) represent pool depths of 1·52 and 2·39 mm, respectively, and curve (*b*) is displaced upward by 3·0 °C.

FIGURE 5. Nield's stability diagram for liquid pools heated from below together with experimental data of the present work: ○, 200 cs. fluid; □, 50 cs. fluid; △, 10 cs. fluid.

| Fluid viscosity (cs.) | Liquid depth (mm) | Critical $\Delta T$ (°C) | $Ma_c$ | $R_c$ | Biot number, $L$ | $Ma^*$ | $R^*$ |
|---|---|---|---|---|---|---|---|
| 200 | 5·72 | 2·63 | 49·4 | 216 | 0·32 | 91·7 | 708 |
| 200 | 6·63 | 2·44 | 54·9 | 323 | 0·41 | 95·0 | 718 |
| 200 | 7·39 | 1·77 | 43·9 | 321 | 0·47 | 97·2 | 725 |
| 200 | 10·29 | 1·20 | 43·7 | 620 | 0·57 | 101 | 735 |
| 50 | 3·81 | 1·54 | 83·7 | 174 | 0·41 | 95·0 | 718 |
| 50 | 4·62 | 1·10 | 73·9 | 226 | 0·47 | 97·2 | 725 |
| 50 | 5·46 | 0·96 | 74 | 310 | 0·34 | 92·4 | 711 |
| 50 | 6·55 | 0·70 | 67 | 420 | 0·64 | 103 | 741 |
| 10 | 1·52 | 0·67 | 99 | 34 | 0·20 | 87·2 | 695 |
| 10 | 2·39 | 0·44 | 100 | 86 | 0·20 | 87·2 | 695 |

TABLE 2. Stability results

Error in the liquid depth measurement did not have a significant effect on the precision with which $Ma_c$ and $R_c$ could be calculated. Even in the very shallow pools with the 10 centistoke oil, the percentage errors in $Ma_c$ and $R_c$ accountable to errors in depth measurement were $\pm 2\,\%$ and $\pm 5\,\%$, respectively.

## 4. Conclusion

For a series of three silicone oils, good agreement existed between the measured and predicted stability criteria for liquid pools heated from below. This appears to be the first quantitative experimental confirmation of the results of the linear hydrodynamic stability analysis that takes surface tension forces into account. Neither deformability of the free surface nor surface active contamination that may have been present had significant effect on the measured stability criteria.

This work was supported in part by the National Science Foundation (Grant number GK-1516).

REFERENCES

BÉNARD, H. 1901 *Ann. Chim. Phys.* **23**, 62.

BERG, J. C. & ACRIVOS, A. 1965 *Chem. Engng. Sci.* **20**, 737.

BERG, J. C., BOUDART, M. & ACRIVOS, A. 1966 In *Advances in Chemical Engineering*, vol. 6, pp. 61–123. (eds. T. B. Drew *et al.*). Academic.

NIELD, D. A. 1964 *J. Fluid Mech.* **19**, 341.

PEARSON, J. R. A. 1958 *J. Fluid Mech.* **4**, 489.

SCHMIDT, R. J. & MILVERTON, S. W. 1935 *Proc. Roy. Soc.* A **152**, 586.

SCRIVEN, L. E. & STERNLING, C. V. 1964 *J. Fluid Mech.* **19**, 321.

SILVESTON, P. L. 1958 *Forsch. Ing. Wes.* **24**, 29, 59.

SPARROW, E. M., GOLDSTEIN, R. J. & JONSSON, V. K. 1964 *J. Fluid Mech.* **18**, 513.